Variation of mechanical properties in a multi-pass weld measured using digital image correlation

Conference or Workshop Item

Presented at SEM Annual Conference, June 1-4, 2009 Albuquerque New Mexico USA

Variation of Mechanical Properties in a Multi-pass Weld Measured Using Digital Image Correlation

M. Acar, S. Gungor*, S. Ganguly, P. J. Bouchard and M. E. Fitzpatrick

Faculty of Mathematics, Computing & Technology
The Open University, Walton Hall
Milton Keynes MK7 6AA, UK

*Corresponding author: s.gungor@open.ac.uk

ABSTRACT

As part of a programme investigating the structural integrity of welds, the Digital Image Correlation (DIC) technique was used to obtain the full-field strain distribution during tensile testing of cross-weld specimens cut from a multi-pass girth welded pipe. The displacement maps were analyzed using Matlab scripts to compute local stress-strain variations from which the local proof stress values were extracted. It has been found that the DIC parameters, such as the size of interrogation windows (subsets) and speckle sizes, have significant effects on the displacement values due to the local variations in the mechanical properties within the weld between the passes. The DIC parameters were therefore optimized using monolithic aluminium alloy specimens with stress concentrations giving similar displacement gradients. The use of a high resolution camera at high magnification allowed the variations between the welding passes to be observed. The variation of the mechanical properties in the weld region is correlated with the full field hardness maps of the same region.

Introduction

The life and structural integrity of engineering structures in power plants operating at high temperatures and pressures is largely governed by the integrity of the welded regions. The understanding and modelling of the mechanical response of welds require knowledge of the variation of mechanical properties in and around the welds. The global response of the welded structure can then be determined by implementing the constitutive stress-strain response in the weld region into numerical modelling codes. The aim of the present study is to develop experimental techniques for determining the mechanical property variations across a weldment from the local stress-strain response obtained by full field strain mapping under tensile loading of standard specimens machined from the weld area.

The digital Image correlation (DIC) technique, which provides full field measurement of surface deformations, has recently been used to study local variations in stress-strain response in samples containing welds [1-5]. Strain maps were obtained on standard tensile specimens that were cut perpendicular to the weld line, such that the gauge length of the specimen contained the fusion zone and the heat affected zone. Kartal *et al*. [1] and Genevois *et al.* [4] also cut micro-tensile test specimens at different regions of welded joint and compared these results with the standard tensile test sample. They found good agreement between the stress-strain data obtained by micro-tensile tests and standard tensile tests.

The working principle of DIC is based on sophisticated computational algorithms that track the grey value patterns in digital images of the test surfaces, taken before and after an event that produces surface deformations, such as

thermal or mechanical loading [7]. The main advantages of the technique are that the test surface requires no, or very little, preparation and the measurements are not affected by rigid body motions.

Typically, digital images of the test surface at different stages of the deformation, captured using high resolution cameras, are processed using custom or commercial software. In this study a commercial image correlation software [6] which employs a Fast Fourier Transform algorithm was used to correlate the images. The determination of displacements is dependent on the existence of random high-contrast patterns, i.e. speckles, on the test surface. The process involves division of each image into sub-regions (subsets or interrogation windows) and a displacement vector is calculated for each subset between each successive images. The strain values are then calculated by differentiating the displacement values for each subset.

The measurement accuracy of the technique depends on many factors, some of which are related to the algorithms used in correlation calculations [8-10]. Furthermore, since the technique is based on the tracking of grey level patterns, the accuracy is largely affected by the size of speckles, the image resolution (i.e. number of pixels per speckle) and the chosen subset size in the calculations [11-13]. In general, subset size should be large enough to have a distinctive intensity pattern. However, the effect of subset size on the accuracy depends on the form of deformation field to be measured. For relatively homogeneous deformations fields, a large subset size is found to give more accurate displacement measurements, as more data points lead to better correlation [11, 12]. But, when the measured deformation field contains high strain gradients, the variation of deformation field within a subset can be considerable if the chosen subset size is too large, which can lead to errors if the deformation field is not accurately approximated with subset shape functions [9,10]. Thus, it seems that smaller subset sizes should be chosen for the measurement of heterogeneous deformation fields. However, the imaging (random) noise becomes more significant with decreasing subset size which affects the accuracy of the measurement [12, 13].

The choice of subset size also depends on the speckle size. The subset should contain sufficient number of speckles in order to have a distinctive intensity pattern. Random speckle patterns are usually applied to test surface by various methods, including spray painting. In this study, it is found that the surface roughness produced by the electro discharge machining (EDM) produces adequate speckle pattern under ordinary white light illumination (Figure 1).

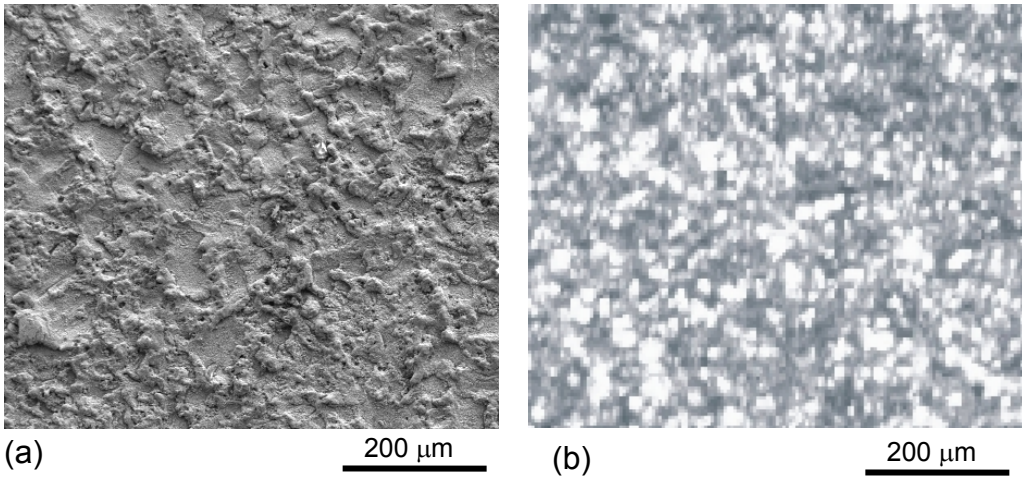

Figure 1 (a) The EDM surface of the aluminium sample (SEM image), and (b) the speckle pattern as captured by the camera under white light illumination (magnified).

The aim of this study was to optimize the parameters used in DIC measurements of welds. Since the mechanical properties around welds show significant variations, the yielding behaviour is expected to be heterogeneous. Therefore, the analysis of welds using DIC requires the parameters discussed above to be optimised for varying strain gradients. A notched tensile sample was used for this purpose. The effect of subset size, speckle size and camera resolution was investigated around the notch stress field where the strain gradient is high and compared to the regions where the deformation is relatively homogeneous. The optimized parameters used to obtain full

field displacement map of tensile test samples that were cut from the weld. The local stress strain curves, extracted from the displacement maps, were then used to determine the variations of proof stress across the weld.

Experimental

Notched tensile aluminium specimen

To optimize the parameters in DIC measurements for varying strain gradients, a notched tensile specimen was used. The specimen was machined from a 2024-T351 aluminium alloy rolled plate using electro discharge machining (EDM). It had a gauge length of 80 mm, width of 10 mm and the thickness of 3 mm. The two semicircular notches with radius of 1.4 mm as shown in Figure 2 gave a theoretical stress concentration factor at their roots as 2.2. The specimen was loaded to six different loads, up to 5.7 kN, using a screw driven tensile testing machine with a calibrated 30 kN capacity load cell. A digital SLR camera (Nikon D300), with a sensor size of 4,288 x 2,848 pixels (12.3 Mega Pixels), and a 200 mm macro lens were used to capture images at each level of loading. The images were analyzed using DIC software to obtain displacement maps at various parameter settings. The displacement data was then used to calculate the axial strain (ε_y) variation between the notches, along the line B in Figure 2. The strain values were calculated by differentiating the displacement data using a Matlab script where the number of neighbouring displacement data points used for the calculation could be specified. The use of fewer data points gives large scatter in the strain values, whereas too many data points may result in smearing out of variation in strain profile. Figure 3 shows an example calculation with data points varying from 3 to 9. Obviously the choice of data points in the calculation depends on the case but, in the case of the notched specimen the use of seven data points seemed to give closest values to the finite element results. Although the displacement maps for all the intermediate loads were obtained, only the strain data for the load 5.7 kN were calculated. At this load, the yield stress was exceeded around the notches while the nominal stress was still elastic. A finite element model of the test sample was constructed to compare the strain distribution with the measurements.

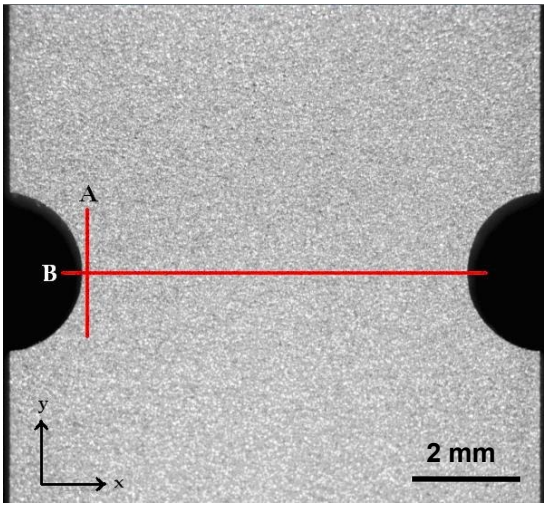

Figure 2 The central section of the notched aluminium specimen.

Cross-weld tensile specimens

The test material for this work was machined from a multi-pass girth-welded ex-service 316H austenitic stainless steel header pipe with 70 mm wall thickness. Two cross-weld tensile specimens, with a gauge length of 70 mm, width of 12 mm and thickness of 3 mm, were cut by EDM from the weld materials as shown in Figure 4. One side of the specimens was metallographicaly polished and electrochemically etched with 60% Nitric acid to reveal the macrostructure of the weld, including the weld-passes. An automated micro hardness tester was used to map the hardness distribution on one of the specimens.

The tension tests on both specimens were performed using a screw driven tensile testing machine with a 30 kN load cell, under constant displacement rate of 0.2 mm/min. The applied load and the cross-head displacement of the testing were recorded. One image of the specimen surface was captured at every 10 seconds during the test using the 12 Mega-pixels camera. The optical magnification was chosen in one test (Test-1) to cover entire gauge length of the specimen, giving a pixel size of ~30 μm. The second specimen (Test-2) was imaged at a higher magnification, a pixel size of ~10 μm, with the aim of capturing strain distribution within individual weld passes. The images were analysed in a similar manner as described for the notched sample.

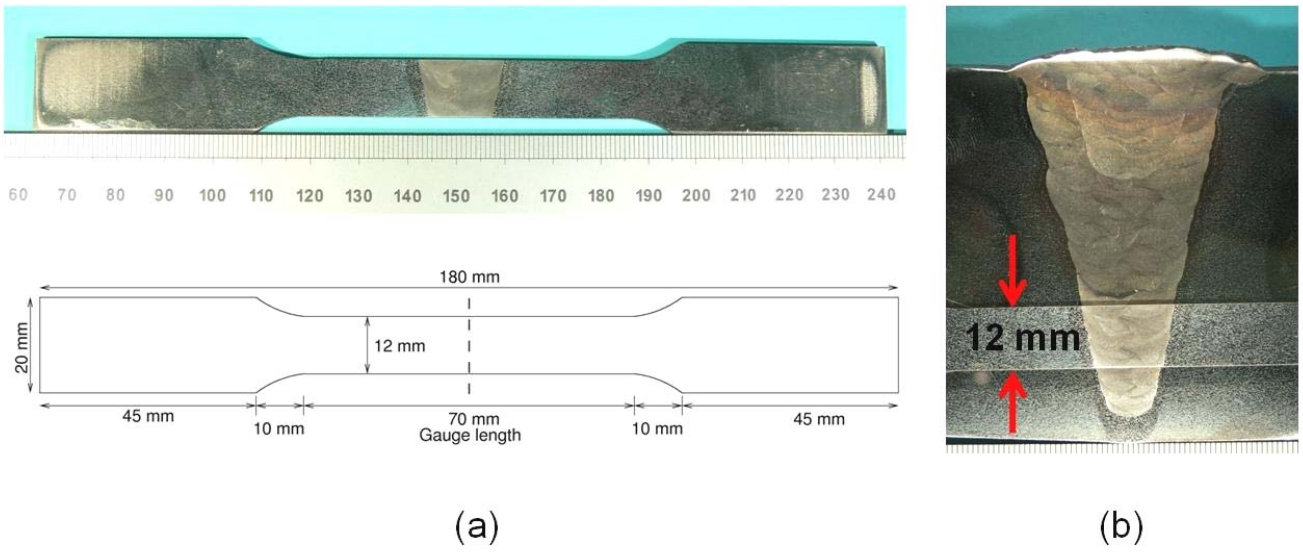

Figure 4 (a) The cross-weld tensile specimen and its dimensions (b) cut position of the specimen with respect to the girth weld.

Results

Notched tensile aluminium specimen

Figure 5 shows the effect of subset size on the variation of axial strain between the notch tips. The measurements are compared to the results obtained by a 2D finite element model based on the specimen dimensions. The material was modelled as elastic – perfectly plastic and a static analysis using plain strain elements was performed for the simulation. It can be seen in Figure 5 that the results obtained with a subset size of 32x32 pixels give the best agreement with the FE results near the notches where the strain gradient is high, whereas the results obtained by 64x64 subset size gives somewhat better fit away from the notches. The strain values for the 16x16 subset size, on the other hand, shows quite a large scatter, although the overall agreement with the FE results can be seen. One of the reasons for the large scatter in the results of 16x16 is that the subset size is smaller than the average speckle size in the images, which is ~20x20 pixels in this case.

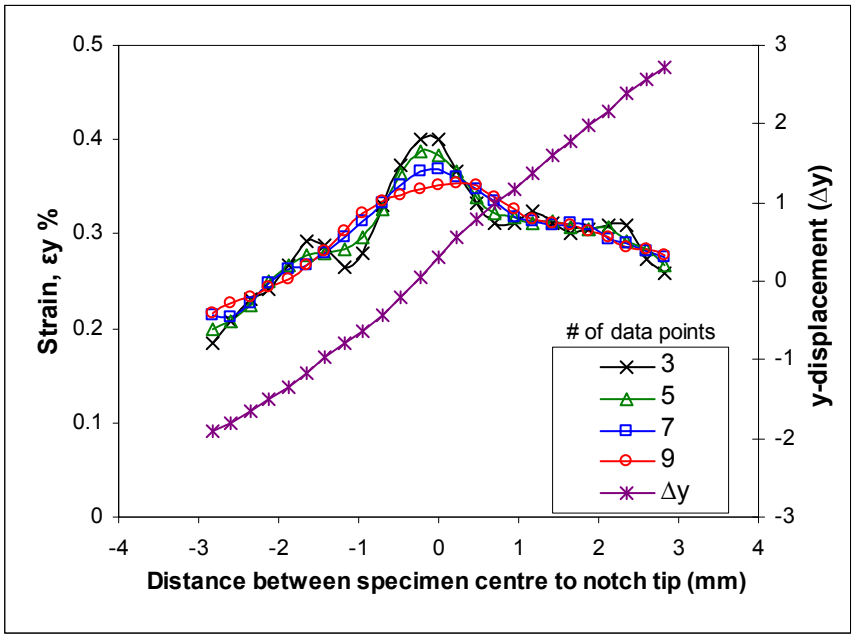

Figure 3 The effect of number of data points in the calculation of strain from the displacement data at the notch tip ('line A' Fig. 2) for subsets of 64x64 pixels.

Although it was not possible to change the speckle size in this study, the effect of speckle size to subset size ratio on the results was investigated by capturing images during the test at various resolution settings on the digital camera. Figure 6 shows that when the number of pixels in an average speckle is halved the scatter in the results for the subset size of 16x16

pixels is reduced. However, the reduction in scatter could not be attributed only to the change in speckle size which was achieved by doubling the effective pixel size in camera settings. Since this process averages the light intensity in a number of neighbouring pixels to produce the new resolution, the noise in the image can be reduced, hence, contributing to a better correlation in displacement calculations.

It should be noted here that the commercial software has some other user defined parameters which significantly influence the results. For example, the correlation calculations can be done iteratively which improves the results. The information of the vector field computed in the first run is used as reference vector field for the next iteration, so that the position of the subset in the new pass is shifted accordingly. This is known to correlate the right speckles and improves the result [6]. Furthermore, using a larger subset size for the first iteration, and then reducing it for the succeeding iterations, has been observed to improve the results. Therefore, in all the reported results here the same number of iterations (i.e. six) and a larger starter subset size (i.e. double the normal size) has been used.

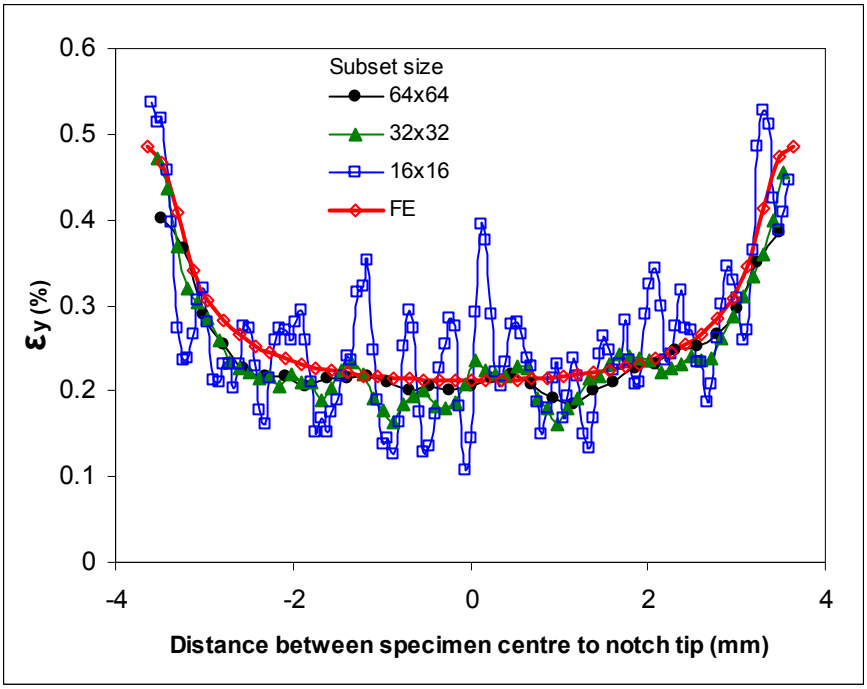

Figure 5 Effect of subset size on strain distribution between the notch tips at the applied load of 5.7kN.

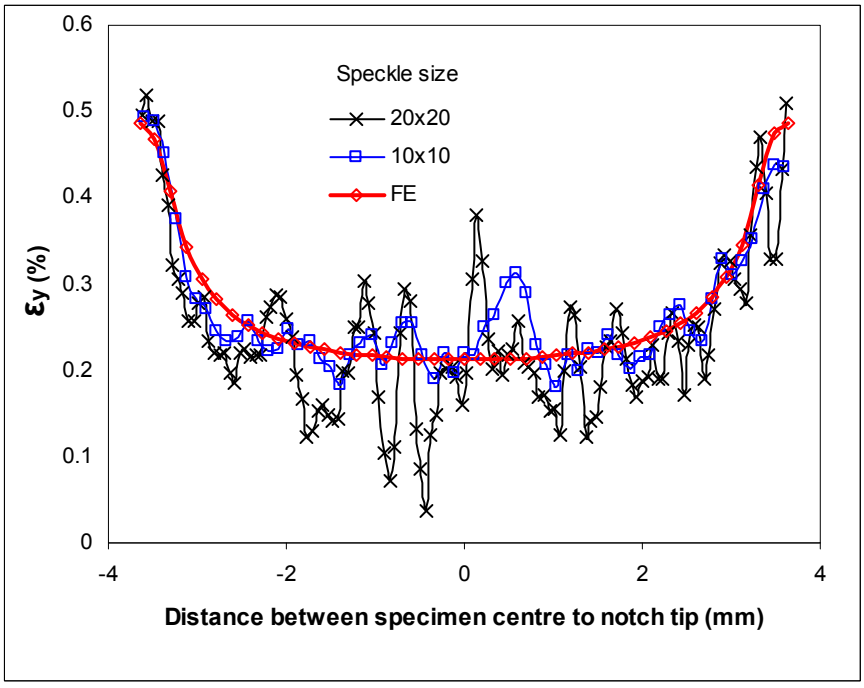

Figure 6 Effect of speckle size on the strain distribution between the notch tips for the subset size of 16x16 pixels.

Cross-weld tensile specimens

Both cross-weld specimens were loaded up to about 15% strain and during each test more than 300 images were captured. Full field displacement maps for the entire set of images were determined and these were then processed to calculate the strain maps. The effect of DIC parameters on strain distributions was also scrutinized. As an example, the effect of subset size for Test-1 (lower magnification images covering entire gauge length) when the sample was loaded to 11.4 kN is shown in Figure 7. The scatter in the results, even for the subset size of 16x16 pixels, is relatively small. This is probably because the average speckle size for this test, about 4x4 pixels, was much smaller than that for the notched specimen. The results in Figure 7 suggests that the subset size 64x64 pixels is probably too large as the

results were relatively smooth, whereas the subset size 16x16 pixels shows the largest scatter, and hence 32x32 pixels seemed to be the best choice in this case.

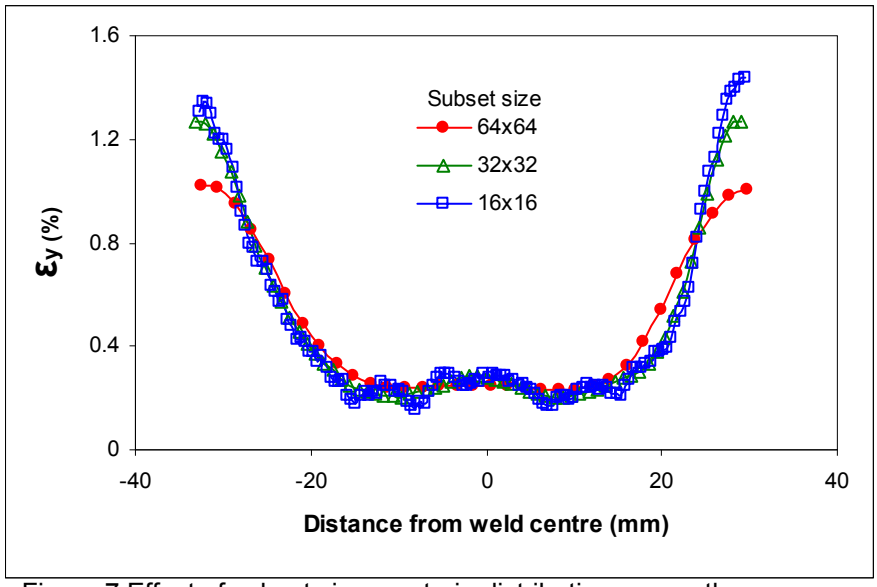

Figure 7 Effect of subset size on strain distribution across the gauge length and at the mid-section of the specimen at a load of 11.4 kN for the low magnification test (Test 1).

As can be seen, the deformation in the weld region, at the centre of the gauge, is comparatively small. The deformation increases with a steep gradient away from the weld region, into the parent material. Although all the subset sizes in Figure 7 seem to give similar strain gradients, there is a considerable difference in the results at the maximum strain, where the deformation levels off in the region of the parent material. Since the mechanical properties of the parent material are known, it was possible to estimate the deformation levels in this region. Examining the local variations of 0.2% proof stress values (which is discussed below) across the gauge length of the specimen, revealed that the results obtained with the subset size 32x32 pixels gives the best agreement with the properties of the parent material.

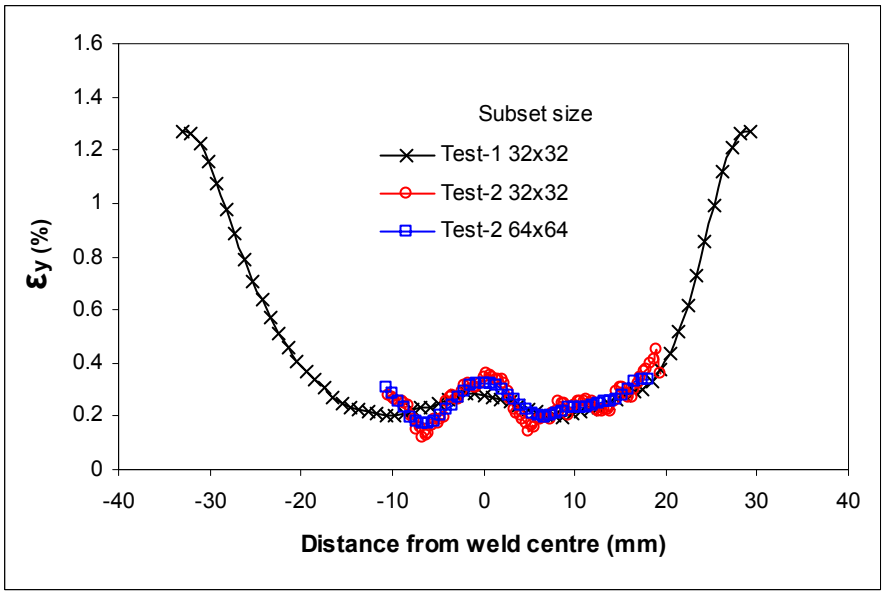

Figure 8 The strain distribution around the weld at the mid-section of the specimen at a load of 11.4 kN for both tests.

The measurements performed at higher optical magnification (Test-2) showed significant variation in strain levels within the weld region. Figure 8 compares, at the same loading level, the results obtained by both tests. The results suggest that the mechanical properties within the welding passes are not uniform. This can be clearly seen in Figure 9 where proof stress variation is plotted as described below. The scatter in Test-2 with the subset size of 32x32 pixels is relatively large, due to the average speckle size of Test 2, 12x12 pixels, is higher than that of Test-1.

The strain values calculated for each subset from the displacement maps were combined with the load data logged with each image captured during the tensile testing, allowing the local stress-strain curves for each subset to be plotted. A Matlab script was written to extract the 0.2% proof stress from each stress-strain curve. Figure 9 shows the variation of proof stress along the gauge length, in the mid-section, of the sample used in Test-1. Clearly, the choice of subset size is critical for revealing the information on underlying deformation around the welding passes. Although there is a reasonable overall agreement between the results obtained by both subset sizes, it is not obvious whether the extra peak observed with the 24x24 subset size is real or artificially created due to scatter in the data. The measurements done at higher magnification with Test-2 were used to scrutinize the strain distribution within the weld. Figure 10 shows the full field map of proof stress within and around the

weld. In the construction of this map, subset size of 64x64 pixels was used to calculate the displacement field. The welding pass boundaries obtained from the macrostructure are superimposed on the proof stress map. The results show two peaks, similar to the ones obtained by the 32x32 pixel subset size in Figure 9. The peaks occur near the weld boundaries, and a significant drop in proof stress is observed towards the weld centre. The Vickers hardness distribution around the weld shown in Figure 11 agrees well with the proof stress calculations.

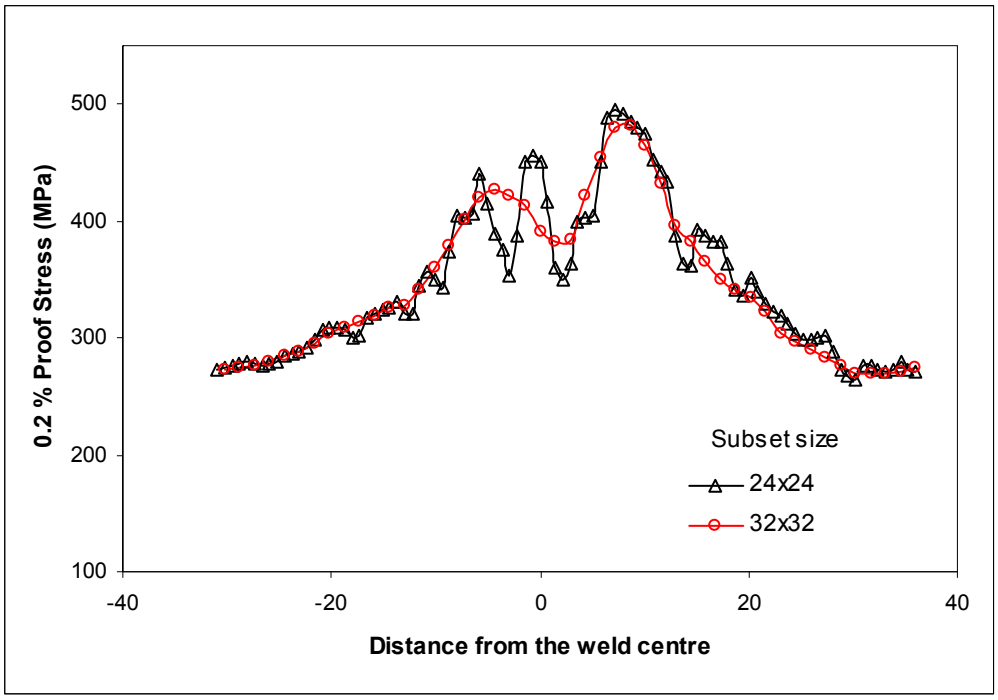

Figure 9 The variation of 0.2% proof stress across the gauge length.

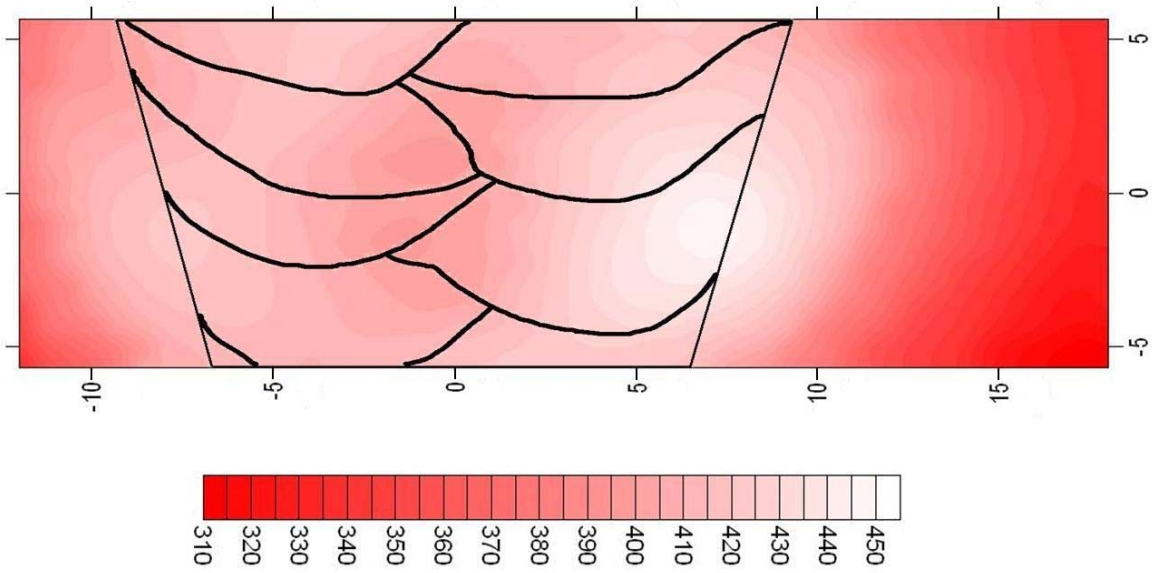

Figure 10 Full field map of 0.2% proof stress on Test-2.

Summary

The effect of digital image correlation parameters on the accuracy of displacement measurements in varying strain gradients was investigated using a notched tensile specimen. It has been observed that a relatively large subset sizes give more accurate displacement measurements when the underlying deformation is homogeneous, whereas smaller subset sizes are required for deformations with steep gradients. Furthermore, the speckle size was found to have critical effect on the accuracy of the results. The optimized parameters were then used to

determine the variation of proof stress across a cross-weld sample taken from a multi-pass girth welded pipe. It has been shown that it was feasible to resolve the variation of strain within the weld-passes with high magnification optical imaging.

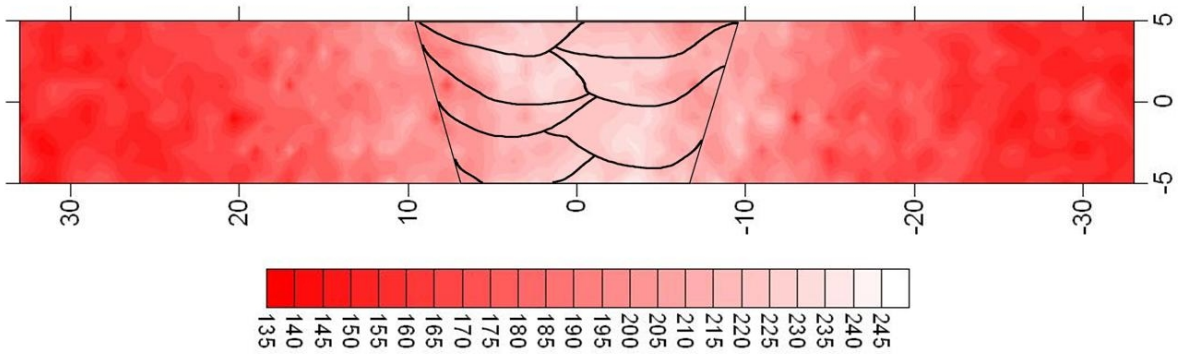

Figure 11 Vickers hardness map on the cross-weld specimen.

Acknowledgements

MA is funded by British Energy, and Dr M Spindler is acknowledged for his support. S Ganguly was funded through the TSEC program KNOO (Keeping the Nuclear Option Open) and as such we are grateful to the EPSRC for funding under grant EP/C549465/1. PJB is supported by a Royal Society Industry Fellowship. MEF is supported by a grant through The Open University from the Lloyd's Register Educational Trust, an independent charity working to achieve advances in transportation, science, engineering and technology education, training and research worldwide for the benefit of all.

References

[1] Kartal M, Molak R, Turski M, Gungor S, Fitzpatrick ME and Edwards L "Determination of Weld Metal Mechanical Properties Utilising Novel Tensile Testing Methods" Applied Mechanics and Materials, 7-8. pp. 127-132 (2007)

[2] Lockwood WD, Tomaz B, and Reynolds AP "Mechanical response of friction stir welded AA2024: experiment and modelling" Materials Sciences and Engineering, A 323, 348-353 (2002)

[3] Sutton MA, Yang B, Reynolds AP and Yan J "Banded microstructure in 2024-T351 and 2524-T351 aluminum friction stir welds: Part II. Mechanical characterization" Materials Sciences and Engineering, A364, 66-74 (2004)

[4] Genevois C, Deschamps A and Vacher P "Comparative study on local and global mechanical properties of 2024 T351, 2024 T6 and 5251 O friction stir welds" Materials Sciences and Engineering, A 415, 162-170 (2006)

[5] Boyce BL, Reu PL and Robino CV Metallurgical and Materials Transaction, 37A, 2481-2492 (2006)

[6] Strain Master, LaVision GmbH, Anna-Vandenhoek-Ring 19, Gottingen, Germany

[7] Sutton MA, McNeill SR, Helm JD and Chao YJ "Advances in two-dimensional and three-dimensional computer vision," in Topics in Applied Physics, 1st ed., P. K. Rastogi, ed., (Springer, Berlin: Springer) p323-372. (2000)

[8] Schreier HW, Braasch JR and Sutton MA "Systematic errors in digital image correlation caused by intensity interpolation," Opt. Eng. 39, 2915-2921 (2000)

[9] Schreier HW and Sutton MA "Systematic errors in digital image correlation due to undermatched subset shape functions," Exp. Mech. 42, 303-310 (2002)

[10] Pan B, Xie HM, Xu BQ, and Dai FL, "Performance of sub-pixel registration algorithms in digital image correlation," Meas. Sci. Technol. 17, 1615-1621 (2006)

[11] Lecompte D, Smits A, Bossuyt Sven, Sol H, Vantomme J and Van Hemelrijck D "Quality assessment of speckle patterns for digital image correlation" Opt. Lasers Eng. 44, 1132-1145 (2006)

[12] Sun YF and Pang HJ "Study of optimal subset size in digital image correlation of speckle pattern images" Opt. Lasers Eng. 45, 967-974 (2007)

[13] Pan B ; Xie H , Wang Z , Qian K and Wang Z, "Study on subset size selection in digital image correlation for speckle patterns," Opt. Express 16, 7037-7048 (2008)